2013

Bis[N-alkyl-NN-di(2-pyridylmethyl)amine]zinc(II) perchlorates display cis-facial stereochemistry in solid state and solution

Lei Zhu, J. Simmons, Zhao Yuan, Kirsten Daykin, Brian Nguyen, Ronald Clark, and Michael Shatruk

Bis[*N*-alkyl-*N*,*N*-di(2-pyridylmethyl)amine]zinc(II) perchlorates display *cis-facial* stereochemistry in solid state and solution

J. Tyler Simmons, Zhao Yuan, Kirsten L. Daykin, Brian T. Nguyen, Ronald J. Clark, Michael Shatruk, and Lei Zhu*

Department of Chemistry and Biochemistry, Florida State University, 95 Chieftan Way, Tallahassee, FL 32306-4390, USA

lzhu@chem.fsu.edu

Bis[*N*-alkyl-*N*,*N*-di(2-pyridylmethyl)amine]zinc(II) perchlorates display *cis-facial* stereochemistry in solid state and solution

N-Alkyl-*N*,*N*-di(2-pyridylmethyl)amines are ligands commonly used by supramolecular chemists in molecular recognition and sensing applications. The metal coordination complexes of these ligands, in particular the ones with 2:1 (ligand:metal) molar ratio, have not been sufficiently characterized in solution. In this work, bis[*N*-alkyl-*N*,*N*-di(2-pyridylmethyl)amine]zinc(II) perchlorates are characterized in both solid and solution phases, using X-ray crystallography and NMR spectroscopy, respectively. Only the c*is-facial* stereoisomer is observed. DFT calculations support the thermodynamic preference for this stereochemistry, as in one representative case the gas phase energy of the *cis-facial* configuration is lower than those of the *trans-facial* and *meridional* configurations by 4.0 and 4.5 kcal/mol, respectively.

Keywords: *cis-facial*; di(2-pyridylmethyl)amine; zinc; HMBC, DFT

Introduction

The syntheses of di(2-pyridylmethyl)amine (DPA) and tris(2-pyridylmethyl)amine (TPA) ligands were reported in the late 1960s (Figure 1),[1] which were soon followed by the studies of their solution metal coordination chemistry.[2] TPA is a high-affinity tetradentate ligand to most first-row transition metal ions.[2b,3] DPA and its *N*-alkylated (or arylated) derivatives are either tridentate or tetradentate (if the added functionality is also coordinating) ligands. Both TPA and DPA derivatives have been invaluable motifs in molecular recognition of metal ions. Their metal complexes have also been used for the detection of anions[4] and neutral molecules.[5]

Similar to the metal coordination complexes of TPA and its derivatives,[6] the complexes of *N*-alkylated DPA derivatives have found broad usage in developing molecular sensors,[7] catalysts,[8] molecular magnetic materials,[9] and chiroptical sensors and switches,[10] by creative selections of the *N*-alkyl groups. The coordination chemistry

of tridentate DPA-derived ligands is, however, more complicated than that of tetradentate TPA, as DPA derivatives are more inclined than TPA to form complexes of 2:1 (ligand:metal) molar ratio with ions of octahedral coordination geometry (Figure 1). Single crystal structures of 2:1 (ligand:metal) complexes of DPA have been known for over two decades,[11] but the solution structural characterizations of these complexes are quite limited at best, relative to, for example, the wide acceptance of DPA derivatives as the receptors of choice in developing fluorescent sensors for metal ions.[7b,12] Herein, we report the characterization of 2:1 (ligand:metal) complexes of different *N*-alkylated DPA ligands with zinc(II) ion, $[Zn(naDPA)_2]X_2$ where X is the counter ion, in acetonitrile using NMR spectroscopy.

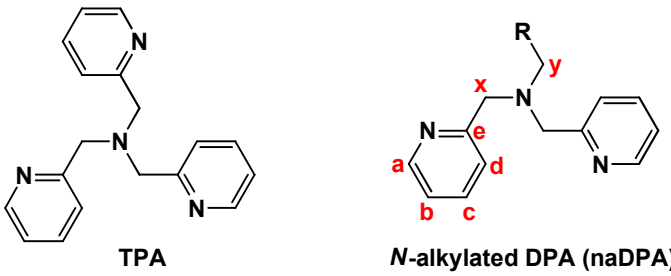

$$TPA + MX_2 \overset{S}{\rightleftharpoons} [M(TPA)(S)]X_2 \text{ and/or } [M(TPA)(X)]X \quad (1)$$

$$naDPA + MX_2 \overset{S}{\rightleftharpoons} [M(naDPA)_2]X_2 \text{ and/or } [M(naDPA)(X)_2] \quad (2)$$

Figure 1. Structures of TPA and an *N*-alkylated DPA (naDPA) derivative. The common coordinative reactions between TPA and naDPA and a divalent metal salt (MX_2) are shown in equations 1 and 2, respectively. X is a monodentate anion. S: solvent that may coordinate monodentately. Although only pentacoordinated structures are represented for the 1:1 (ligand:metal) complexes, hexacoordinated structures are also known.

In a previous work from our group,[13] DPA derivative **1** was characterized to form a stable 2:1 (ligand:Zn) complex (Figure 2) as a single stereoisomer (racemic) by

both single crystal X-ray diffractometry in solid state and ^{1}H NMR spectroscopy in solution (CD_3CN). Complex $[Zn(\mathbf{1})_2](ClO_4)_2$ shows *cis-facial* stereochemistry with C_2 symmetry, which is one of the three possible stereoisomers of a 2:1 (ligand:metal) complex with an acyclic tridentate ligand having two identical terminals (Figure 3).[11b] This singular stereochemical outcome is shared by the few $[Zn(naDPA)_2]X_2$ complexes of which the crystal structures have been reported.[14]

The solution structure of $[Zn(\mathbf{1})_2](ClO_4)_2$ replicates that in the solid state.[13] The two 2-pyridylmethyl groups on one DPA ligand are no longer in the same chemical environment. They were preliminarily assigned as the axial (red in Figure 2 in the online version) and equatorial (blue in the online version) 2-pyridylmethyl groups. The assignment of the ^{1}H NMR spectrum of $[Zn(\mathbf{1})_2](ClO_4)_2$ was based primarily on the ^{1}H COSY data, with the assistance from the crystal structure.

The observation of a single stereoisomer of $[Zn(\mathbf{1})_2](ClO_4)_2$ in solution was unanticipated. This outcome shall be the consequence of the thermodynamic preference for the *cis-facial* stereochemistry because zinc(II) ion is kinetically labile. To determine whether this preference holds regardless of the *N*-alkyl substituent, the 2:1 (ligand:Zn) complexes of several other *N*-alkylated DPA derivatives are characterized in the current work using ^{1}H NMR spectroscopy. Improving upon the previous work,[13] the carbon-carbon connectivities of the complex are now directly established using the heteronuclear multiple quantum coherence (HMQC) and heteronuclear multiple bond coherence (HMBC) techniques. The chemical shift difference between the two sets of 2-pyridylmethyl groups is rationalized with more confidence. Finally, DFT calculations provide further support for the stereochemical preference of the *cis-facial* isomer in these complexes.

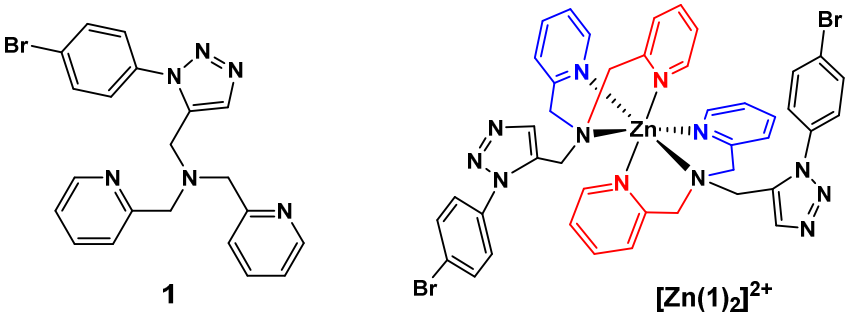

Figure 2. Structures of tridentate DPA derivative **1** and the cationic portion of its 2:1 complex with zinc(II).

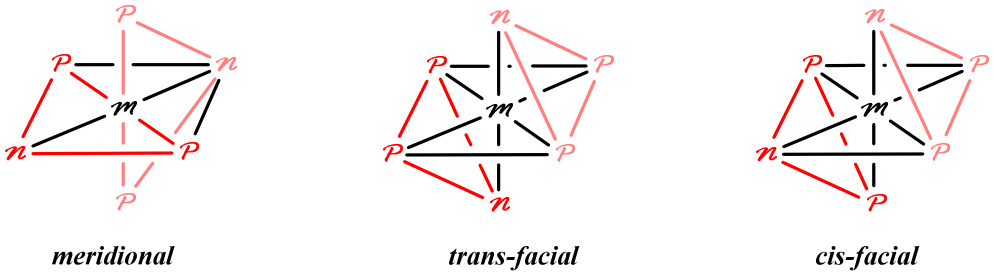

Figure 3. Three possible stereoisomers of $[ML_2]^{2+}$, adapted from reference #11b. Enantiomers are not included. The planes defined by the two ligands are shown in colour in the online version. L = p-n-p, a neutral DPA derivative such as compound **1**. p: pyridyl; n: amino.

Results and Discussion

(1) Synthesis

There are two synthetic routes to access *N*-alkylated DPA derivatives that have been wide applied (Scheme 1).[15] S_N2 substitution between DPA and *n*-octylbromide, propargyl bromide, and 9-(chloromethyl)anthracene produces ligands **2**,[8a] **4**,[15a] and **5**,[15a] respectively. Reductive amination between DPA and *p*-chlorobenzaldehyde affords ligand **3**. The full procedures and characterization data are included in the Experimental Section.

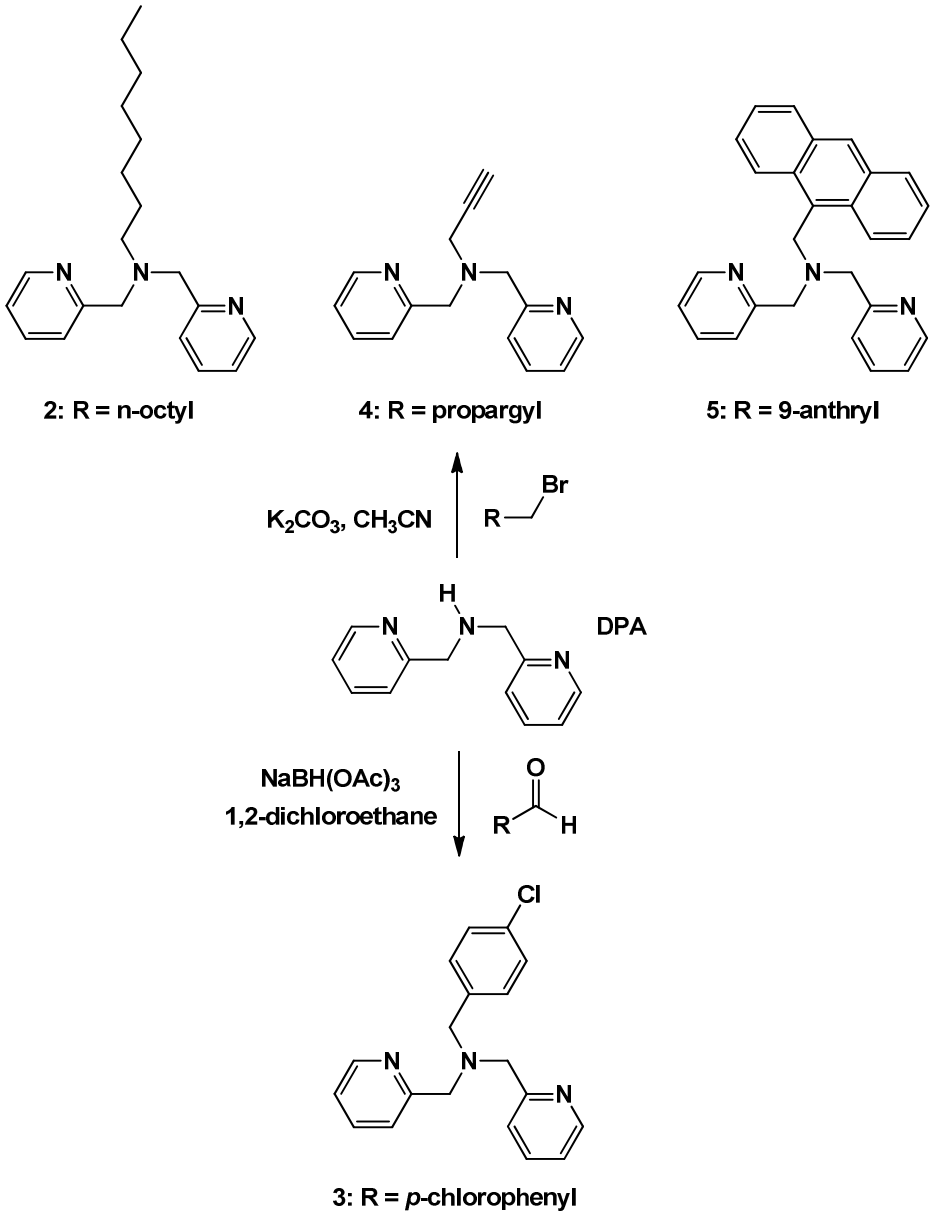

Scheme 1. Synthesis of the *N*-alkylated DPA ligands **2**-**5**.

(2) X-ray single crystal structures of the 2:1 (ligand:Zn) complexes

Similar to the synthesis of $[Zn(\mathbf{1})_2](ClO_4)_2$,[13] the 2:1 (ligand:Zn) complexes were prepared by mixing a ligand and $Zn(ClO_4)_2 \cdot 6H_2O$ at the 2:1 molar ratio in acetonitrile. Upon solvent removal, the crude complex was rinsed with diethyl ether and vacuum dried. The solid material was then redissolved in a minimal amount of acetonitrile. Slow

diffusion of diethyl ether into the acetonitrile solution afforded the single crystals of $[Zn(\mathbf{3})_2](ClO_4)_2$ and $[Zn(\mathbf{5})_2](ClO_4)_2$ within 2 days.

The cationic part of the published complex $[Zn(\mathbf{1})_2](ClO_4)_2$[13] is redrawn in Figure 4a for comparison purposes. The atoms pertinent to the current discussion are labelled. The complex has a *cis-facial* stereochemistry with C_2 symmetry. The two pyridyl groups of **1** are not chemically equivalent in $[Zn(\mathbf{1})_2](ClO_4)_2$, and are designated as equatorial (eq) and axial (ax) pyridyls. Other labels follow the numbering scheme defined in Figure 1, and apostrophes are used to identify the protons on axial pyridyls.

The crystal structure of complex $[Zn(\mathbf{3})_2](ClO_4)_2$ is shown in Figure 4b (non-coordinating ClO_4^- anions are omitted). There are two crystallographically independent molecules in the unit cell, but the difference between them has no impact on the conclusion of this work. Both molecules have *cis-facial* stereochemistry, consistent with that of $[Zn(\mathbf{1})_2](ClO_4)_2$[13] and other reported crystal structures of $[Zn(naDPA)_2]X_2$ complexes.[14]

Complex $[Zn(\mathbf{5})_2](ClO_4)_2$ replicates the *cis-facial* stereochemistry. Ligand **5** is one of the earliest examples of fluorescence sensors based on metal coordination-switchable intramolecular photoinduced electron transfer.[7a,16] This compound is also arguably the first one that was considered as a fluorescent sensor for zinc(II) ions following the development of the TSQ class of compounds.[17] The DPA ligand has subsequently been included in many fluorescent sensors targeting zinc(II) ions.[12] The current work offers for the first time the structural characterization of the 2:1 (ligand:Zn) complex of ligand **5**.

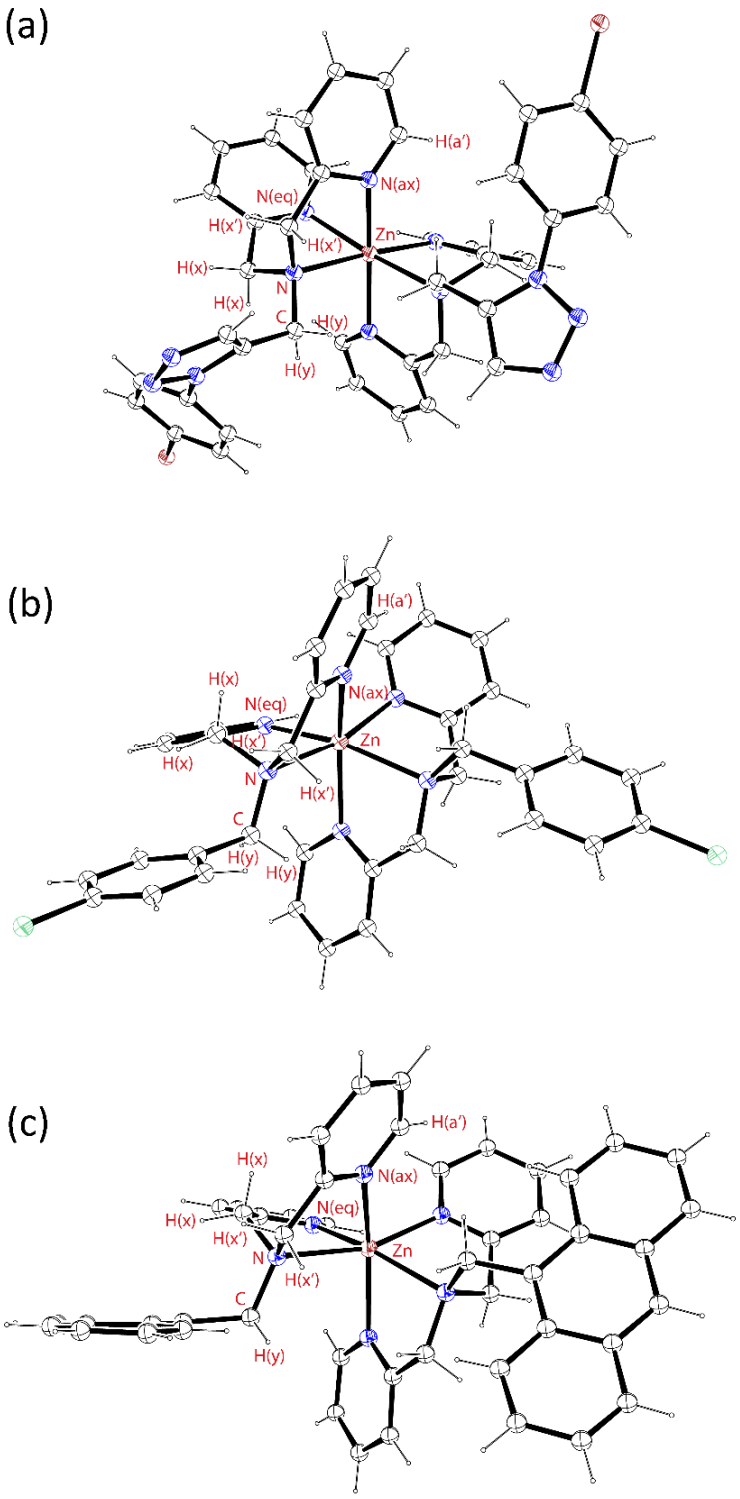

Figure 4. Cationic portions of the crystal structures of (A) $[Zn(\mathbf{1})_2](ClO_4)_2$. Selected bond distances: N(eq)-Zn = 2.171(2) Å; N(ax)-Zn = 2.105(2) Å; N-Zn = 2.247(2) Å; (B) $[Zn(\mathbf{3})_2](ClO_4)_2$. Selected bond distances: N(eq)-Zn = 2.115(3) Å; N(ax)-Zn = 2.171(2) Å; N-Zn = 2.293(2) Å; (C) $[Zn(\mathbf{5})_2](ClO_4)_2$. Selected bond distances: N(eq)-Zn = 2.129(2) Å; N(ax)-Zn = 2.187(2) Å; N-Zn = 2.341(2) Å. H, C: black; N: blue; Br: brown; Cl: green. The colours are shown in the online version.

(3) ^{1}H NMR (600 MHz, CD_3CN) studies

The ^{1}H NMR spectra of ligands **2**-**4** and their 2:1 and 1:1 (ligand:Zn) complexes in CD_3CN were acquired. The trend of shifting of the ^{1}H NMR signals upon zinc(II) coordination is similar for all ligands. Therefore, only the spectra of ligand **4** and its complexes are shown in Figures 5-6, and discussions on Zn(II)-induced spectral changes are made specific to ligand **4**. The 2D NMR spectra of 2:1 (ligand:Zn) complexes of other ligands are included in the Supporting Information. The pyridyl (a-d, see numbering in Figure 1) and methylene (x-y) protons of ligands **1**-**4** and their 2:1 and 1:1 complexes are tabulated in Tables 1, 2, and 3, respectively.

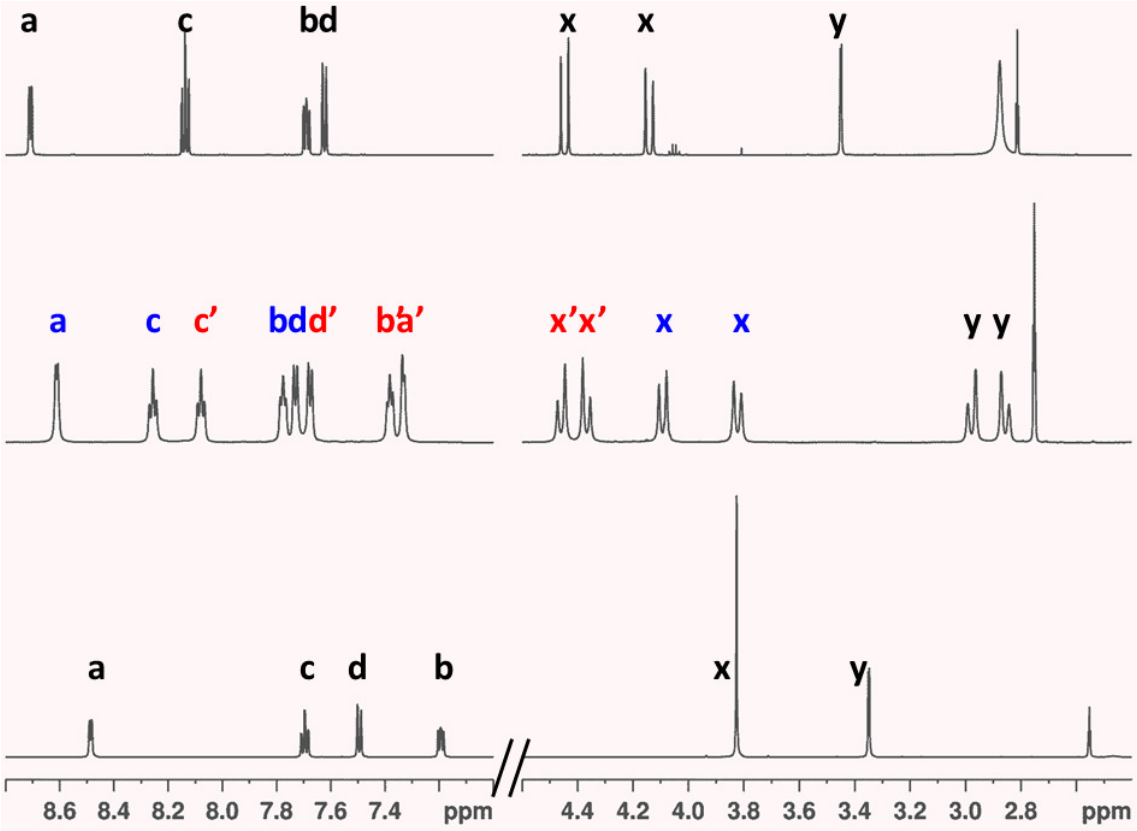

Figure 5. ^{1}H NMR (600 MHz, CD_3CN) spectra of (bottom) ligand **4**, (middle) $[Zn(\mathbf{4})_2](ClO_4)_2$, and (top) $[Zn(\mathbf{4})(CD_3CN)_2](ClO_4)_2$.[18] For $[Zn(\mathbf{4})_2](ClO_4)_2$ (middle), regular letters represent equatorial pyridyl, while apostrophes identify the axial pyridyl (see later sections for stereochemical assignments).

The ^{1}H NMR spectrum of ligand **4** (Figure 5, bottom) shows the two 2-pyridylmethyl groups to be chemically equivalent. The pyridyl and propargyl methylenes (x and y in Figure 1) are singlets at 3.83 and 3.35 ppm, respectively. Among the four pyridyl protons, H(a) (8.49 ppm) and H(c) (7.70 ppm), which are respectively *ortho* and *para* to the pyridyl nitrogen atom, are downfield shifted from H(d) (7.50 ppm) and H(b) (7.19 ppm).

Upon forming the 1:1 complex (Figure 5, top), all the proton signals (a-d, x-y) shift downfield to various degrees. The downfield shifts are expected because the positively charged zinc(II) ion deshields the protons via the inductive effect. The methylene protons H(x) next to the 2-pyridyl are now non-equivalent, as they are part of the kinetically stable 5-membered coordination rings.[13] Therefore, two doublets for two H(x)'s are observed. This pattern of chemical shift redistribution of the DPA ligand upon forming a 1:1 (ligand:metal) complex is well-documented by us[15a] and others.[19]

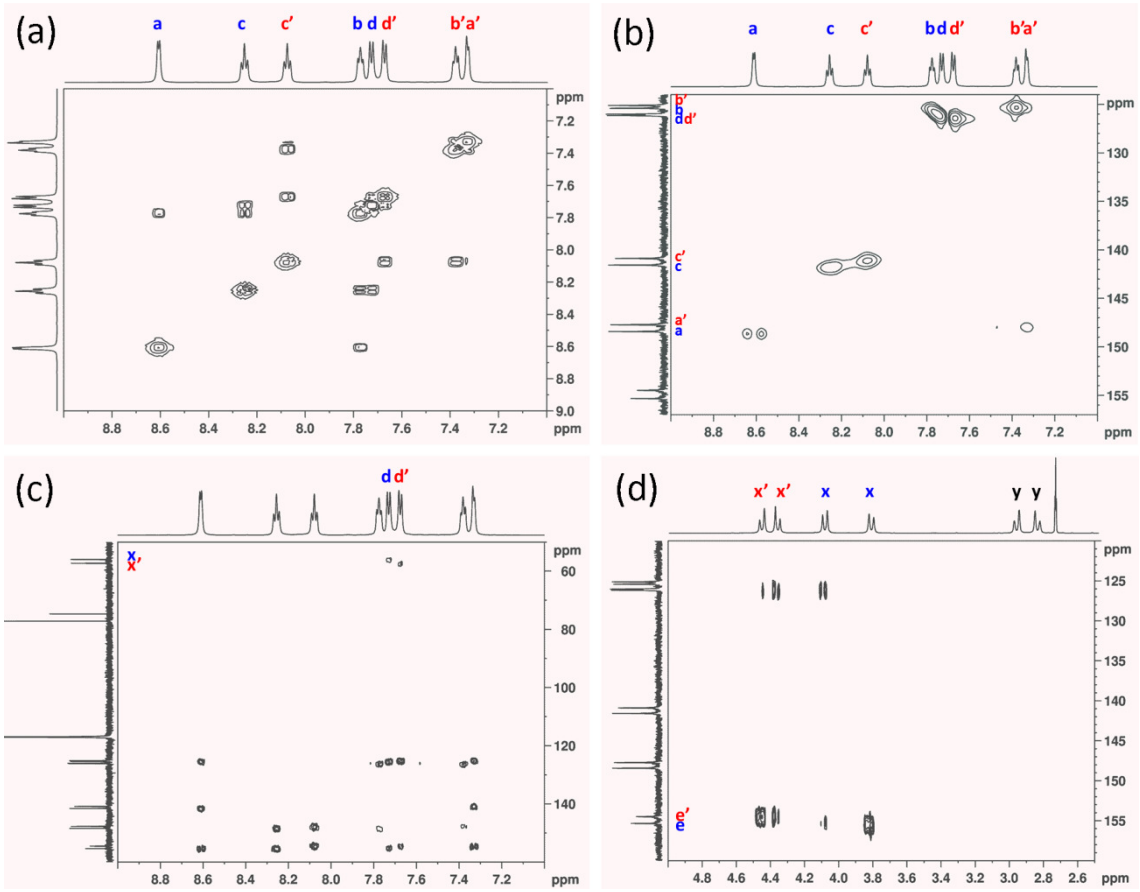

Figure 6. (a) ^{1}H COSY, (b) HMQC spectra of $[Zn(\mathbf{4})_2](ClO_4)_2$ of the aromatic region, (c) and (d) HMBC spectra of $[Zn(\mathbf{4})_2](ClO_4)_2$ showing the correlations of ^{13}C to aromatic or aliphatic ^{1}H, respectively. Regular letters represent equatorial pyridyl, while apostrophes identify the axial pyridyl (see later sections for stereochemical assignments).

The ^{1}H NMR of the 2:1 (ligand:Zn) complex, $[Zn(\mathbf{4})_2](ClO_4)_2$, reveals 8 aromatic and 6 aliphatic protons that are integrated equally (Figure 5, middle), which indicates that the two 2-pyridylmethyl groups are no longer chemically equivalent. Two sets of pyridyl protons (a-d and a'-d') are distinguished based on ^{1}H COSY data (Figure 6a). Protons H(a')-H(d') are consistently upfield shifted from their counterparts H(a)-H(d) in the other set. Remarkably, H(a') is the most shielded among all aromatic protons at 7.30 ppm, a significant departure from H(a), which is found at 8.58 ppm, the most deshielded of all.

The signals in the ^{13}C NMR spectrum are assigned using the HMQC technique. The aromatic portion of the HMQC spectrum is shown in Figure 6b. Five pairs of aromatic carbons are identified (left vertical axis), confirming that the two pyridyl groups (5 carbons each) are no longer chemically equivalent. Carbon signals C(a')-C(d') are slightly, but consistently upfield shifted from their counterparts, C(a)-C(d). The quaternary carbons C(e) and C(e') are assigned using the HMBC technique (vide infra).

The connectivities between the methylene and 2-pyridyl groups across the quaternary C(e) and C(e') are established using the HMBC technique, which shows long range (2-3 bonds) ^{1}H-^{13}C correlations. As shown in Figure 6c, C(x) and C(x') are assigned via respective cross peaks to H(d) and H(d'), a three-bond correlation. The protons H(x) and H(x') (labelled in Figure 5, middle) are subsequently assigned via ^{1}H-^{13}C correlations in the HMQC spectrum (the relevant portion is shown in Figure S1, Supporting Information). The remaining two aliphatic doublets are therefore assigned to diastereotopic protons H(y) (labelled in Figure 5b). The quaternary carbons C(e) and C(e') are now assigned via HMBC correlations to protons H(x) and H(x'), respectively (Figure 6d).

Table 1. 2-Pyridylmethyl ^{1}H NMR (600 MHz, CD_3CN) chemical shifts (ppm) in free ligands **1**-**4**.[a]

	a	b	c	d	x	y
1[b]	8.43	7.19	7.62	7.16	3.69	3.85
2	8.45	7.16	7.67	7.53	3.72	2.45
3	8.46	7.18	7.70	7.55	3.72	3.62
4	8.49	7.19	7.70	7.50	3.83	3.35

a. See labelling (a-d, x-y) in Figure 1; b. data taken from ref. #13.

Table 2. 2-Pyridylmethyl ^{1}H NMR (600 MHz, CD_3CN) chemical shifts (ppm) in the 2:1 (ligand:Zn) complexes.[a] Ligand = **1**-**4**.

	a	a'	b	b'	c	c'	d	d'	x	x'	y
1[b]	8.49	7.22	7.65	7.42	7.98	8.06	6.87	7.65	3.46; 3.42	4.52; 4.31	3.24; 3.20
2	8.68	7.31	7.76	7.31	8.21	8.0	7.67	7.6	4.06; 3.68	4.35; 4.32	1.89
3	8.76	7.52	7.83	7.35	8.30	7.97	7.79	7.52	3.83; 3.47	4.71; 4.01	3.06
4	8.58	7.30	7.75	7.35	8.23	8.05	7.70	7.65	4.06; 3.79	4.43; 4.34	2.95; 2.83

a. See labelling (a-d, x-y) in Figure 1. Protons on axial and equatorial 2-pyridylmethyl groups are color-coded red and blue in the online version, respectively. See later sections for stereochemical assignments; b. data taken from ref. #13.

Table 3. 2-Pyridylmethyl ^{1}H NMR (600 MHz, CD_3CN) chemical shifts (ppm) in the 1:1 (ligand:Zn) complexes.[a] Ligand = **1**-**4**.

	a	b	c	d	x	y
1[b]	8.65	7.65	8.03	7.22	4.02; 3.87	3.97
2	8.73	7.67	8.11	7.58	4.32; 4.05	2.67
3	8.75	7.70	8.15	7.59	4.26; 3.83	3.78
4	8.71	7.69	8.14	7.63	4.45; 4.14	3.45

a. See labelling (a-d, x-y) in Figure 1; b. data taken from ref. #13.

After both ^{1}H and ^{13}C NMR spectra of $[Zn(\mathbf{4})_2](ClO_4)_2$ have been fully analysed based on bond connectivity (COSY, HMQC, and HMBC), the final challenge is to assign the two sets of 2-pyridylmethyl groups in the *cis-facial* isomer that is universally observed in $[Zn(naDPA)_2]X_2$ complexes.[14] As shown in $[Zn(\mathbf{1})_2](ClO_4)_2$ (Figure 2), the two pyridyl groups in each ligand are designated as axial and equatorial (red and blue,

respectively, in the online version), which are referred hereupon as ax-pyridyl and eq-pyridyl groups, respectively. A few observations from the connectivity assignment that might aid the stereochemical assignment of ax- and eq-pyridyls are: (1) protons H(a')-H(d') are shielded relatively to protons H(a)-H(d), and the shielding of H(a') is remarkable. (2) Protons H(y) are consistently upfield shifted comparing to those in the free ligand. (3) Protons H(x') are deshielded compared to H(x). (4) These observations are consistent in the 2:1 (ligand:Zn) complexes of all ligands studied (see Table 2). Therefore, the shielding or deshielding of the protons depends little on the identity of the *N*-substituent.

In the previously reported $[Zn(\mathbf{1})_2](ClO_4)_2$, the upfield shifted set of pyridyl protons H(a')-H(d') were assigned to the ax-pyridyls.[13] The shielding of ax-pyridyls was attributed to the presence of the 1-(4'-bromophenyl)-1,2,3-triazolyl group. Herein, we confirm the previous ^{1}H NMR assignment of $[Zn(\mathbf{1})_2](ClO_4)_2$ with respect to ax- and eq-pyridyls. However, contrary to the explanation provided previously, we conclude that the chemical shift differences between ax- and eq-pyridyls, or the shielding of the ax-pyridyl, shall not be entirely attributed to the influence of the *N*-alkyl groups.

The following discussion explains how the assignment of the shielded set of protons H(a')-H(d') to ax-pyridyls is consistent with the four key observations listed earlier.

- In the crystal structures shown in Figure 4, proton H(a') on an ax-pyridyl always locates above the equatorial pyridyl ring of the other ligand, which shall provide a strong shielding magnetic anisotropy effect to H(a').
- The folded, fused two 5-membered coordination rings in the facial ligand dictate that the N-C bond connecting to the alkyl group is parallel to the

ax-pyridyl group of the other ligand (Figure 4). The ax-pyridyl group consequently shields protons H(y) in all 2:1 (ligand:Zn) complexes, which explains the consistent upfield shifts of protons H(y) comparing to their counterparts in the free ligands. These two observations are the direct ramifications of the *cis-facial* stereochemistry of the 2:1 (ligand:Zn) complex, regardless of the identity of the *N*-alkyl group.

- The equatorial methylene protons (H(x) in Figure 4) are closer to the *N*-alkyl group in the same ligand than the axial methylenes (H(x')). Therefore, Protons H(x) are more shielded by the *N*-alkyl group in the same ligand than protons H(x'). This shielding effect does depend on the nature of the *N*-alkyl group. As listed in Table 2, the aryl ring-containing alkyl groups in ligands **1** and **3** lead to larger upfield shifts of protons H(x) in the 2:1 (ligand:Zn) complexes than the shifts of protons H(x) of ligands **2** and **4** without an aromatic substituent.

Based on these arguments, we complete the ^{1}H NMR assignment of the 2:1 (ligand:Zn) complexes, which is tabulated in Table 2, and graphically represented by the spectrum of $[Zn(\mathbf{4})_2](ClO_4)_2$ in Figure 5, middle.

(4) Computational studies

To elucidate the relative stability of the *cis-facial* isomer with respect to the other possible geometrical configurations, we carried out electronic structure calculations of $[Zn(\mathbf{1})_2]^{2+}$ at the DFT level of theory, using the B3LYP exchange-correlation functional and the LanL2DZ basis set to simulate the experimental conditions. The DFT calculations reveal that the stability of the *cis-facial* isomer of $[Zn(\mathbf{1})_2]^{2+}$ in the gas phase exceeds those of the *trans-facial* and the *meridional* isomers by 4.0 and 4.5 kcal/mol, respectively. These energy differences translate into the

corresponding equilibrium constants of 8.4×10^2 and 1.9×10^3, respectively, indicating the essentially quantitative thermodynamic prevalence of the *cis-facial* isomer at room temperature (Table 4). Smaller, yet substantial favourability to the *cis-facial* isomer is still observed when solvation in acetonitrile is considered (Table 4).

Table 4. Calculated relative energies (kcal/mol) of three stereoisomers of $[Zn(\mathbf{1})_2]^{2+}$.

	cis-fac	*trans-fac*	*mer*	$K_{trans\text{-}fac \rightarrow cis\text{-}fac}$	$K_{mer \rightarrow cis\text{-}fac}$
$[Zn(\mathbf{1})_2]^{2+}$ (gas)	0	4.0	4.5	8.4×10^2	1.9×10^3
$[Zn(\mathbf{1})_2]^{2+}$ (solv)[a]	0	3.5	3.9	3.2×10^2	7.4×10^2

a. solv: assuming the complex exists in acetonitrile solution (conducting polarizable continuum (CPCM) solvation model).

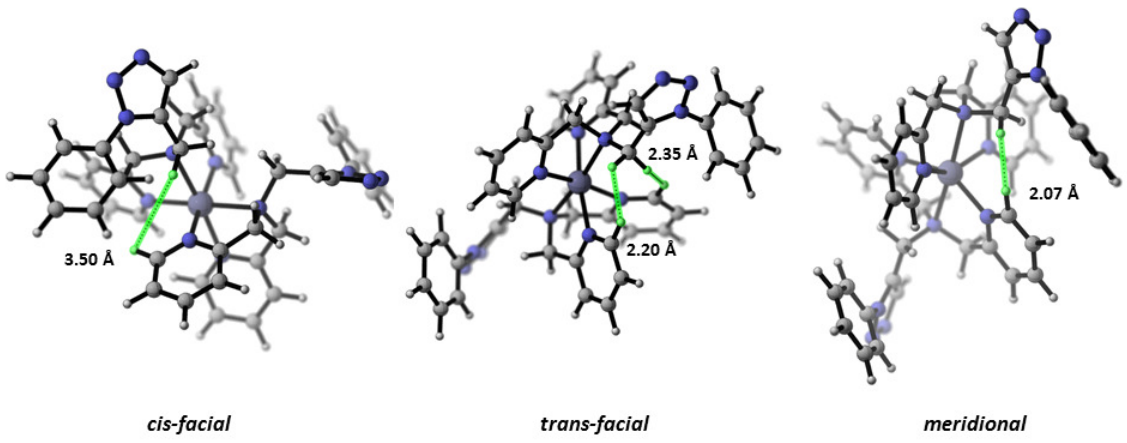

Figure 7. DFT calculated structures (B3LYP/LanL2DZ) of the three stereoisomers of $[Zn(\mathbf{1})_2]^{2+}$. The shortest *interligand* distances between selected H(y) and H(a) hydrogen atoms in each structure are highlighted in green in the online version, and in-focus. The images were created using the CYLview program.[20]

The calculated structures (Figure 7) of the three stereoisomers of $[Zn(\mathbf{1})_2]^{2+}$ reveal subtle but important differences that shed light on the observed selectivity of the

cis-facial isomer. A key difference among the three stereoisomers is the distance between the H(y) methylene hydrogens (see Figure 1 for labelling) of one ligand and the H(a) pyridyl hydrogens of the other ligand. For clarity, only one of the two identical steric interactions is highlighted in the structures shown in Figure 7. The distances between these two hydrogen atoms in both the *trans-facial* and the *meridional* isomers are shorter than in the *cis-facial* isomer, indicating an increased steric interaction between the methylene and pyridyl groups. The least stable *meridional* isomer possesses the closest interligand H(y)-H(a) distance at 2.07 Å, while the *trans-facial* isomer contains two steric interactions between one set of H(y) methylene hydrogens and two separate pyridyl rings with distances of 2.20 and 2.35 Å. The shortest interligand H(y)-H(a) distance in the *cis-facial* isomer is 3.50 Å. Therefore, the instability of the *trans-facial* and *meridional* isomers may be attributed to the steric interligand interactions in the 2:1 (ligand:Zn) complex between the *N*-alkyl group and pyridyl groups.

Conclusion

N-Alkyl-*N*,*N*-di(2-pyridylmethyl)amine ligands are widely used as key components for molecular recognition by supramolecular chemists. These ligands are capable of forming metal coordination complexes in both 2:1 and 1:1 (ligand:metal) molar ratios. In this work, we report the structural characterizations in both solid state and solution of 2:1 (ligand:Zn) complexes of *N*-alkyl-*N*,*N*-di(2-pyridylmethyl)amines. In both states, only the *cis-facial* stereoisomer has been observed, which suggests the thermodynamic preference to this stereoisomer among the three possibilities. The DFT calculations support the thermodynamic favourability to the *cis-facial* isomer over the *trans-facial* and *meridional* isomers. The thermodynamic dominance of the *cis-facial* stereoisomer is attributed to its lack of *N*-alkyl/pyridyl steric interaction, which is

present in the other two isomers, as revealed in the DFT-optimized structures. The 2:1 (ligand:metal) complexes of DPA-derived ligands have not been investigated in solution as extensively as the 1:1 complexes, although they almost always form when the ligand-to-metal ratio is larger than 1. The current work provides the solution structural information on these complexes, which shall not only aid the future studies on their properties, but can also explain the occasional unexpected observations in spectroscopic data of metal-coordinated fluorescent ligands with different ligand-to-metal molar ratios.[29]

Experimental Section

(1) Materials and general methods

Reagents and solvents were purchased from various commercial sources and used without further purification unless otherwise stated. All reactions were carried out in an inert atmosphere of argon. Analytical thin-layer chromatography (TLC) was performed using pre-coated TLC plates with silica gel 60 F254 (EMD) or with aluminium oxide 60 F254 neutral (EMD). Flash column chromatography was performed using 40-63 μm (230-400 mesh ASTM) silica gel (EMD). Silica gel was flame-dried under vacuum to remove adsorbed moisture before use. NMR spectra were recorded on a 600 MHz Bruker AVANCE III NMR Spectrometer. All chemical shifts were reported in δ units relative to tetramethylsilane. High resolution mass spectra were obtained at the Mass Spectrometry Laboratory at FSU. Elemental analysis data were collected at Atlantic Microlab, Inc. Compounds **1** and **4** was reported previously.[13]

(2) Syntheses and characterizations

Compound 2. Di(2-picolyl)amine (0.50 mmol, 100 mg), CH_3CN (3 mL), K_2CO_3 (2.36 mmol, 325 mg), and 1-bromooctane (0.70 mmol, 135 mg) were added to a round-bottom flask and stirred at rt for 3 days. The reaction mixture was then diluted with ethyl acetate and filtered through a pad of K_2CO_3. The crude product was further purified via an alumina gel column by eluting with a 50/50 mixture of ethyl acetate and CH_2Cl_2 to give compound **2** in 52% yield (83 mg). ^{1}H NMR (600 MHz, CD_3CN): δ/ppm 8.45 (d, J = 4.9 Hz, 2H), 7.67 (td, J = 7.7, 1.8 Hz, 2H), 7.53 (d, J = 7.9 Hz, 2H), 7.16 (t, J = 5.6 Hz, 2H), 3.72 (s, 4H), 2.45 (t, J = 7.2 Hz, 2H), 1.48 (pent, J = 7.4 Hz, 2H), 1.28-1.12 (m, 10H), 0.84 (t, J = 7.1 Hz, 3H); ^{13}C NMR (150 MHz, CD_3CN): δ/ppm 160.1, 148.6, 136.1, 122.7, 121.8, 60.2, 53.9, 31.5, 29.0, 28.9, 26.9, 26.8, 22.3, 13.4; HRMS (CI) (*m*/*z*): $[M+H]^+$ calcd for $C_{20}H_{30}N_3$ 312.24397, found 312.24261.

Compound 3. 4-chlorobenzaldehyde (1.0 mmol, 156 mg), 1,2-dichloroethane (2.5 mL), di(2-picolyl)amine (1.04 mmol, 208 mg), and sodium triacetoxyborohydride (1.15 mmol, 244 mg) were added to a round-bottom flask and stirred overnight under argon. The reaction mixture was then diluted with ethyl acetate and a saturated $NaHCO_3$ solution (1 mL). The mixture was washed with saturated $NaHCO_3$ (3 × 50 mL), dried over anhydrous Na_2SO_4, and concentrated under reduced pressure. The crude product was purified via a silica gel column by eluting with ethyl acetate in CH_2Cl_2 (50%, 100 mL), followed by 1-2% CH_3OH (50 mL) in CH_2Cl_2 to give pure compound **3** in 73% yield (236 mg). ^{1}H NMR (600 MHz, CD_3CN): δ/ppm 8.46 (d, J = 4.5 Hz, 2H), 7.70 (td, J = 5.9, 1.7 Hz, 2H), 7.55 (d, J = 7.9 Hz, 2H), 7.40 (d, J = 8.5 Hz, 2H), 7.31 (d, J = 8.4 Hz, 2H), 7.18 (t, J = 6.5 Hz, 2H), 3.72 (s, 4H), 3.62 (s, 2H); ^{13}C NMR (150 MHz, CD_3CN): δ/ppm 159.0, 148.3, 137.7, 135.8, 131.5, 129.9, 127.6, 122.2, 121.5, 59.0, 56.6; HRMS (CI) (*m*/*z*): $[M+H]^+$ calcd for $C_{19}H_{19}N_3Cl$ 324.12675, found 324.12697.

Compound 5.[22] 9-(Chloromethyl)anthracene (1.2 mmol, 272 mg), CH_3CN (6 mL), K_2CO_3 (4.7 mmol, 650 mg), and di(2-picolyl)amine (1.0 mmol, 200 mg) were added to a round-bottom flask and stirred at rt overnight under argon. The reaction mixture was then diluted with ethyl acetate and filtered before it was concentrated under reduced pressure. The pure product was then obtained by recrystallization in a cold solution of CH_2Cl_2 and hexanes in 73% yield (286 mg). ^{1}H NMR (600 MHz, CD_3CN): δ/ppm 8.46-8.42 (m, 5H), 8.02-8.00 (m, 2H), 7.61 (td, J = 7.7, 1.8 Hz, 2H), 7.50-7.45 (m, 4H), 7.31 (d, J = 7.8 Hz, 2H), 7.16-7.14 (m, 2H), 4.67 (s, 2H), 3.82 (s, 4H).

Complex $[Zn(3)_2](ClO_4)_2$. A stock solution of compound **3** in CH_3CN (0.3 mL, 0.335 mM, 0.1 mmol) was added to a small vial followed by $Zn(ClO_4)_2{\cdot}6H_2O$ (18.6 mg, 0.05 mmol). The reaction mixture was stirred ~10 min before it was concentrated under reduced pressure. The resulting complex was then washed with diethyl ether three times before it was vacuum dried. The complex was redissolved in a small amount of CH_3CN and filtered through a pad of glass microfiber. Slow diffusion of diethyl ether into the CH_3CN solution afforded single crystals suitable for X-ray diffraction within 2 days. Anal. calcd for $C_{40}H_{39}Cl_4N_7O_8Zn$ (M + CH_3CN): C, 50.41; H, 4.12; N, 10.29, found: C, 50.68; H, 4.15; N, 9.78.

Complex $[Zn(5)_2](ClO_4)_2$ was prepared using the same procedure as described above for preparing $[Zn(\mathbf{3})_2](ClO_4)_2$. Anal. calcd for $C_{56}H_{49}Cl_2N_7O_8Zn$ (M + CH_3CN): C, 62.03; H, 4.56; N, 9.04, found: C, 62.21; H, 4.71; N, 9.23.

(3) Single crystal X-ray crystallography

Crystal data collection and refinement. A suitable single crystal was mounted on a goniometer head of a Bruker SMART APEX II diffractometer using a nylon loop with a small amount of Paratone oil (Hampton Research). The crystal was cooled to either 103 K ($[Zn(\mathbf{3})_2](ClO_4)_2$) or 203 K ($[Zn(\mathbf{5})_2](ClO_4)_2$ in a cold stream of N_2 gas.

After a crystal that was indexed to give a satisfactory unit cell was found, a full, low-temperature data set was recorded using a sample-to-detector distance of 6 cm. The number of frames taken was typically 2400 using 0.3° ω scans with 20-s of frame collection time. Data integration was performed using the program SAINT, which is part of the Bruker suite of programs.[23] Empirical absorption correction was performed using SADABS.[24] XPREP was used to obtain an indication of the space group, and the structure was solved by direct methods and refined by SHELXTL.[25] All non-hydrogen atoms were fined anisotropically, while hydrogen atoms were typically placed in calculated positions and constrained to a riding model.

$[Zn(3)_2](ClO_4)_2$ (CCDC 947701). The crystal is monoclinic with a P2(1)/c space group. The asymmetric unit consists of two $[Zn(\mathbf{3})_2]^{2+}$ ions, four perchlorate ions and one acetonitrile solvent molecule. The two molecules have the same metal-ligand connectivity but different conformations. For instance, the phenyl groups are arranged at somewhat different angles in the two molecules. Also, the chlorine atoms in one molecule have noticeably more disorder than those in the other. There is, in addition, some disorder in the perchlorate ions, but not nearly as much as one often sees.

$[Zn(5)_2](ClO_4)_2$ (CCDC 947702). The structure was determined at 203 K. There is a low temperature phase change starting at a little above 170 K that changes the nature of the reflections and clearly will change the structure. The details have not yet been determined. The crystal is octahedral with an Fdd2 space group. The asymmetric unit consists of $[Zn(\mathbf{5})_2]^{2+}$ ion, one of the two required perchlorate counter ions and an acetonitrile solvent molecule. The material is moderately stable in air. A small oil coated crystal could still be indexed after four days in Florida's humid air although the quality had clearly deteriorated.

(4) Theoretical studies

DFT calculations were performed with the Gaussian 09 package,[26] using the B3LYP hybrid functional[27] and the LanL2DZ basis set.[28] The starting geometries for the *cis-facial* isomer were taken from the refined crystal structure parameters. The starting geometries for the *trans-facial* and *meridional* isomers were generated by applying standard symmetry elements to modify the symmetry of the *cis-facial* isomer. All geometries were optimized in the ground state without symmetry restraints, using the conducting polarized continuum medium (CPCM, CH_3CN) solvation model to include solvent polarization effects.

Acknowledgements. This work was supported by grants from the US National Science Foundation to L.Z. (CHE-1213574) and M.S. (CHE-0911109).

References

(1) (a) Romary, J. K.; Bunds, J. E.; Barger, J. D. *J. Chem. Eng. Data* **1967**, *12*, 224; (b) Anderegg, G.; Wenk, F. *Helv. Chim. Acta* **1967**, *50*, 2330.

(2) (a) Romary, J. K.; Barger, J. D.; Bunds, J. E. *Inorg. Chem.* **1968**, *7*, 1142; (b) Anderegg, G.; Hubmann, E.; Podder, N. G.; Wenk, F. *Helv. Chim. Acta* **1977**, *60*, 123.

(3) (a) Allen, C. S.; Chuang, C.-L.; Cornebise, M.; Canary, J. W. *Inorg. Chim. Acta* **1995**, *239*, 29; (b) Blackman, A. *Polyhedron* **2005**, *24*, 1.

(4) (a) O'Neil, E. J.; Smith, B. D. *Coord. Chem. Rev.* **2006**, *250*, 3068; (b) Kruppa, M.; König, B. *Chem. Rev.* **2006**, *106*, 3520; (c) Sakamoto, T.; Ojida, A.; Hamachi, I. *Chem. Commun.* **2009**, 141; (d) Kim, S. K.; Lee, D. H.; Hong, J.-I.; Yoon, J. *Acc. Chem. Res.* **2009**, *42*, 23; (e) Ngo, H. T.; Liu, X.; Jolliffe, K. A. *Chem. Soc. Rev.* **2012**, *41*, 4928.

(5) (a) Rosenthal, J.; Lippard, S. J. *J. Am. Chem. Soc.* **2010**, *132*, 5536; (b) Royzen, M.; Wilson, J. J.; Lippard, S. J. *J. Inorg. Biochem.* **2012**, *118*, 162.

(6) (a) Dai, Z.; Canary, J. W. *New J. Chem.* **2007**, *31*, 1708; (b) Liang, J.; Zhang, J.; Zhu, L.; Duarandin, A.; Victor G. Young, Jr.; Geacintov, N.; Canary, J. W. *Inorg. Chem.* **2009**, *48*, 11196.

(7) (a) de Silva, S. A.; Zavaleta, A.; Baron, D. E.; Allam, O.; Isidor, E. V.; Kashimura, N.; Percapio, J. M. *Tetrahedron Lett.* **1997**, *38*, 2237; (b) de Silva, A. P.; Moody, T. S.; Wright, G. D. *Analyst* **2009**, *134*, 2385.

(8) (a) Xia, J.; Matyjaszewski, K. *Macromolecules* **1999**, *32*, 2434; (b) Bergbreiter, D. E.; Hamilton, P. N.; Koshti, N. M. *J. Am. Chem. Soc.* **2007**, *129*, 10666; (c) Mortezaei, S.; Catarineu, N. R.; Canary, J. W. *J. Am. Chem. Soc.* **2012**, *134*, 8054.

(9) Buchen, T.; Hazell, A.; Jessen, L.; McKenzie, C. J.; Nielsen, L. P.; Pedersen, J. Z.; Schollmeyer, D. *J. Chem. Soc., Dalton Trans.* **1997**, 2697.

(10) (a) Zahn, S.; Canary, J. W. *Science* **2000**, *288*, 1404; (b) Canary, J. W.; Mortezaei, S.; Liang, J. *Chem. Commun.* **2010**, *46*, 5850; (c) Carney, P.; Lopez, S.; Mickley, A.; Grinberg, K.; Zhang, W.; Dai, Z. *Chirality* **2011**, *23*, 916.

(11) (a) Butcher, R. J.; Addison, A. W. *Inorg. Chim. Acta* **1989**, *158*, 211; (b) Glerup, J.; Coodson, P. A.; Hodgson, D. J.; Michelsen, K.; Nielsen, K. M.; Wehela, H. *Inorg. Chem.* **1992**, *31*, 4611; (c) Velusamy, M.; Palaniandavar, M.; Thomas, K. R. J. *Polyhedron* **1998**, *17*, 2179; (d) Hazell, A.; McKenzie, C. J.; Nielsen, L. P. *Polyhedron* **2000**, *19*, 1333.

(12) Xu, Z.; Yoon, J.; Spring, D. R. *Chem. Soc. Rev.* **2010**, *39*, 1996.

(13) Simmons, J. T.; Allen, J. R.; Morris, D. R.; Clark, R. J.; Levenson, C. W.; Davidson, M. W.; Zhu, L. *Inorg. Chem.* **2013**, *52*, 5838.

(14) (a) Banthia, S.; Samanta, A. *Eur. J. Org. Chem.* **2005**, 4967; (b) Maity, B.; Gadadhar, S.; Goswami, T. K.; Karande, A. A.; Chakravarty, A. R. *Dalton Trans.* **2011**, *40*, 11904; (c) Mikata, Y.; Fujimoto, T.; Fujiwara, T.; Kondo, S.-i. *Inorg. Chim. Acta* **2011**, *370*, 420.

(15) (a) Huang, S.; Clark, R. J.; Zhu, L. *Org. Lett.* **2007**, *9*, 4999; (b) Zhang, L.; Clark, R. J.; Zhu, L. *Chem. Eur. J.* **2008**, *14*, 2894; (c) Michaels, H. A.; Murphy, C. S.; Clark, R. J.; Davidson, M. W.; Zhu, L. *Inorg. Chem.* **2010**, *49*, 4278.

(16) (a) Zhu, L.; Zhang, L.; Younes, A. H. *Supramol. Chem.* **2009**, *21*, 268; Ligand **5** was included in a fluorescent heteroditopic ligand targeting zinc(II) ions. See: (b) Wandell, R. J.; Younes, A. H.; Zhu, L. *New J. Chem.* **2010**, *34*, 2176.

(17) (a) Frederickson, C. J.; Kasarskis, E. J.; Ringo, D.; Frederickson, R. E. *J. Neurosci. Methods* **1987**, *20*, 91; (b) Nasir, M. S.; Fahrni, C. J.; Suhy, D. A.; Kolodsick, K. J.; Singer, C. P.; O'Halloran, T. V. *J. Biol. Inorg. Chem.* **1999**, *4*, 775.

(18) Perchlorate counter ion may coordinate to zinc(II) instead of CD_3CN.

(19) Goforth, S. K.; Walroth, R. C.; McElwee-White, L. *Inorg. Chem.* **2013**, *52*, 5692.

(20) CYLview, 1.0b; Legault, C. Y., Université de Sherbrooke, 2009 (http://www.cylview.org).

(21) Kim, Y.; Park, B. K.; Eom, G. H.; Kim, S. H.; Park, H. M.; Choi, Y. S.; Jang, H. G.; Kim, C. *Inorg. Chim. Acta* **2011**, *366*, 337.

(22) Ojida, A.; Mito-oka, Y.; Inoue, M.-a.; Hamachi, I. *J. Am. Chem. Soc.* **2002**, *124*, 6256.

(23) SMART and SAINT; Bruker AXS Inc.: Madison, WI, **2007**.

(24) SADABS; Bruker AXS Inc.: Madison, WI, **2001**.

(25) Sheldrick, G. M. *Acta Crystallogr. Sect. A* **2008**, *A64*, 112.

(26) *Gaussian 03, Revision C.02* M. J. Frisch, G. W. Trucks, H. B. Schlegel, G. E. Scuseria, M. A. Robb, J. R. Cheeseman, J. A. Montgomery, Jr., T. Vreven, K. N. Kudin, J. C. Burant, J. M. Millam, S. S. Iyengar, J. Tomasi, V. Barone, B. Mennucci, M. Cossi, G. Scalmani, N. Rega, G. A. Petersson, H. Nakatsuji, M. Hada, M. Ehara, K. Toyota, R. Fukuda, J. Hasegawa, M. Ishida, T. Nakajima, Y. Honda, O. Kitao, H. Nakai, M. Klene, X. Li, J. E. Knox, H. P. Hratchian, J. B. Cross, V. Bakken, C. Adamo, J. Jaramillo, R. Gomperts, R. E. Stratmann, O. Yazyev, A. J. Austin, R. Cammi, C. Pomelli, J. W. Ochterski, P. Y. Ayala, K. Morokuma, G. A. Voth, P. Salvador, J. J. Dannenberg, V. G. Zakrzewski, S. Dapprich, A. D. Daniels, M. C. Strain, O. Farkas, D. K. Malick, A. D. Rabuck, K. Raghavachari, J. B. Foresman, J. V. Ortiz, Q. Cui, A. G. Baboul, S. Clifford, J. Cioslowski, B. B. Stefanov, G. Liu, A. Liashenko, P. Piskorz, I. Komaromi, R. L. Martin, D. J. Fox, T. Keith, M. A. Al-Laham, C. Y. Peng, A. Nanayakkara, M. Challacombe, P. M. W. Gill, B. Johnson, W. Chen, M. W. Wong, C. Gonzalez, and J. A. Pople, Gaussian, Inc., Wallingford CT, **2004**.

(27) (a) Becke, A. D. *Phys. Rev. A* **1988**, *38*, 3098; (b) Lee, C.; Yang, W.; Parr, R. G. *Phys. Rev. A* **1988**, *37*, 785.

(28) (a) Dunning, T. H., Jr.; Hay, P. J. *Mod. Theor. Chem.* **1977**, *3*, 1; (b) Hay, P. J.; Wadt, W. R. *J. Chem. Phys.* **1985**, *82*, 270; (c) Hay, P. J.; Wadt, W. R. *J. Chem. Phys.* **1985**, *82*, 299; (d) Wadt, W. R.; Hay, P. J. *J. Chem. Phys.* **1985**, *82*, 284.

(29) See an example in reference #15c.